

# Caspase-11 Mediates Oligodendrocyte Cell Death and Pathogenesis of Autoimmune-mediated Demyelination

By Shin Hisahara,\* Junying Yuan,<sup>§</sup> Takashi Momoi,<sup>||</sup> Hideyuki Okano,\*<sup>‡</sup> and Masayuki Miura\*<sup>‡¶</sup>

From the \*Division of Neuroanatomy, Department of Neuroscience, Osaka University Graduate School of Medicine, Osaka 565-0871, Japan; the <sup>‡</sup>Core Research for Evolutional Science and Technology (CREST), Osaka 565-0871, Japan; the <sup>§</sup>Department of Cell Biology, Harvard Medical School, Boston, Massachusetts 02115; the <sup>||</sup>Division of Development and Differentiation, National Institute of Neuroscience, Tokyo 187-8502, Japan; and the <sup>¶</sup>Laboratory for Cell Recovery Mechanisms, Brain Science Institute, RIKEN, Saitama 351-0198, Japan

## Abstract

Multiple sclerosis (MS) and its animal model, experimental autoimmune encephalomyelitis (EAE), are inflammatory diseases of the central nervous system (CNS) characterized by localized areas of demyelination. The mechanisms underlying oligodendrocyte (OLG) injury in MS and EAE remain unknown. Here we show that caspase-11 plays crucial roles in OLG death and pathogenesis in EAE. Caspase-11 and activated caspase-3 were both expressed in OLGs in spinal cord EAE lesions. OLGs from caspase-11-deficient mice were highly resistant to the cell death induced by cytotoxic cytokines. EAE susceptibility and cytokine concentrations in the CNS were significantly reduced in caspase-11-deficient mice. Our findings suggest that OLG death is mediated by a pathway that involves caspases-11 and -3 and leads to the demyelination observed in EAE.

Key words: apoptosis • cytokines • experimental autoimmune encephalomyelitis • multiple sclerosis • knockout mouse

## Introduction

Multiple sclerosis (MS)<sup>1</sup> and its animal model, experimental autoimmune encephalomyelitis (EAE), are T cell-mediated inflammatory diseases of the central nervous system (CNS). Although apoptosis in EAE lesions has been reported, the mechanism that leads to oligodendrocyte (OLG) injury remains to be determined (1, 2). We have generated transgenic mice that express the baculovirus antiapoptotic, caspase-inhibitory protein p35 in OLGs through the Cre-*loxP* system (3). p35-expressing OLGs derived from transgenic mice were resistant to cytotoxic cytokine-induced cell death. These mice were also resistant to EAE induction by immunization with the myelin OLG glycoprotein (MOG). The number of activated caspase-3-expressing and apoptotic OLGs was reduced in

the white matter of the lumbar spinal cord. Thus, the inhibition of caspases in OLGs prevents them from undergoing cell death and ameliorates the severity of autoimmune demyelinating diseases. These findings raised questions about how caspase-3 is activated and whether its activation is critical for the pathogenesis of MS and EAE. Previously, a reduction in the incidence and severity of EAE was observed in caspase-1 knockout mice (4). However, the precise role of caspase-1 in EAE, especially with regard to OLG cell death, largely remains to be elucidated because caspase-11 expression is eliminated in caspase-1 knockout mice for unclear reasons (5).

Murine caspase-11 is a member of the caspase-1 subfamily (6) and is required for caspase-1-induced apoptosis and IL-1 $\beta$  secretion (7). Physical interaction between caspase-11 and caspase-1 is a critical step in the activation of caspase-1 (7). Recent findings have shown that the substrate specificity of caspase-11 is similar to caspase-9, and that caspase-11 can promote the processing of caspase-3, suggesting that caspase-11 works as the apical caspase in the cascade that activates downstream executioner caspases under pathological conditions (5). These findings suggest that the activation of caspase-11 leads to the processing of both

Address correspondence to Masayuki Miura, Laboratory for Cell Recovery Mechanisms, Brain Science Institute, RIKEN, 2-1 Hirosawa, Wako, Saitama 351-0198, Japan. Phone: 81-48-467-6945; Fax: 81-48-467-6946; E-mail: miura@brain.riken.go.jp

<sup>1</sup>Abbreviations used in this paper: ALP, alkaline phosphatase; CNS, central nervous system; EAE, experimental autoimmune encephalomyelitis; FBS, fetal bovine serum; GST, glutathione S-transferase; IGIF, IFN- $\gamma$  inducing factor; MBP, myelin basic protein; MOG, myelin OLG glycoprotein; MS, multiple sclerosis; OLG, oligodendrocyte.

caspase-1 and -3. In this context, caspase-11 is thought to be crucial in both inflammation and apoptosis in certain pathological conditions. Because inflammation and OLG injury are characteristic for MS and EAE, we expect that caspase-11 plays pivotal roles in the progression of MS and EAE.

In this study, we examined the role of caspase-11 in OLG death in EAE. Caspase-11 is highly expressed in both OLGs and infiltrating cells such as T lymphocytes in EAE lesions. Although the number of OLGs was reduced in EAE lesions, the proportion of apoptotic OLGs that expressed activated caspase-3 was increased compared with spinal cord tissue from wild-type mice. The colocalization of caspase-11 and activated caspase-3 in the OLGs suggests that a pathway involving caspase-11 and -3 is important in the execution of OLG death in EAE lesions. *In vitro*, cell death induced by TNF- $\alpha$ , IFN- $\gamma$ , or anti-Fas antibody, and the activation of caspase-3 by TNF- $\alpha$  and IFN- $\gamma$  were all reduced in caspase-11-deficient OLGs, indicating that caspase-11 functions in a cell-autonomous manner to regulate cell death. Caspase-11-deficient mice were significantly resistant to the induction of EAE immunized with MOG peptide. In a histopathological study of caspase-11-deficient mice, the number of activated caspase-3-expressing and apoptotic OLGs was markedly decreased. Furthermore, the concentrations of IL-1 $\beta$  and IFN- $\gamma$  were also reduced in the CNS, indicating the non-cell-autonomous mechanism of caspase-11 in regulating the inflammatory process. Our results suggest that caspase-11 plays a pivotal role in the execution of OLG death and the neurological manifestations of MS and EAE.

## Materials and Methods

**Mice.** The caspase-11<sup>-/-</sup> and caspase-11<sup>+/-</sup> mice were described previously (7). These heterozygous and homozygous knockout mice have been maintained as a breeding colony at Osaka University for ~3 yr. They were backcrossed for at least five generations, usually eight generations, into C57BL/6 background mice. 8-wk-old male and female C57BL/6 mice and 8–12-wk-old female C57BL/6 mice in a late stage of pregnancy were obtained from Charles River Laboratories.

**Induction and Assessment of EAE.** The Animal Welfare Guidelines of Osaka University Medical School were followed for all studies and experiments with mice. The procedure used to induce EAE was described previously (3). In brief, mice were immunized with CFA (Difco) supplemented with 100  $\mu$ g of rat MOG<sub>35–55</sub> peptide, and synthesized by Biologica with 4 mg/ml *Mycobacterium tuberculosis* H37Ra (Difco). All C57BL/6 mice received a subcutaneous injection of peptide in 0.1 ml of sterilized PBS in the footpads of both hind feet. Immediately afterwards, each mouse was also injected with 300 ng pertussis toxin (List Biological) in 0.25 ml PBS intravenously; this injection was repeated 48 h after the immunization. Clinical signs of disease were graded on a scale of 0 to 6, with 0.5 points for intermediate clinical findings, as follows: 0, normal; 1, weakness of the tail; 2, complete loss of tail tonicity or abnormal gait; 3, partial hind limb paralysis; 4, complete hind limb paralysis; 5, forelimb paralysis or moribund; and 6, death.

**Western Blotting Analysis.** Cervical/thoracic, and lumbar spi-

nal cords from control and EAE mice 20 d after immunization were washed with PBS, homogenized in assay buffer (50 mM Tris-HCl, pH 7.4, 1 mM EDTA, and 10 mM EGTA), and then frozen immediately. After adding 10  $\mu$ M digitonin, the homogenate was incubated at 37°C for 10 min. The homogenate was clarified by centrifugation at 15,000 rpm for 10 min. The clear supernatant fraction was used for immunoblotting. Equal amounts of protein (~15  $\mu$ g) from the spinal cords were loaded on each lane of a 12.5% polyacrylamide gel for SDS-PAGE. After electrophoresis, proteins were transferred onto an Immobilon-P membrane (Millipore). Immunoblotting was carried out using rat monoclonal anti-caspase-1 and -11 antibodies (a 1:100 dilution in 4% skim milk; reference 7), a rabbit polyclonal anti-caspase-3 antibody (1:1,000 dilution; a gift from Dr. J.L. Goldstein, University of Texas Southeastern Medical Center, Dallas, TX; reference 8), and a mouse monoclonal anti-caspase-8 antibody (MBL; 1:500 dilution). Anti-rat, -rabbit, and -mouse IgGs conjugated with alkaline phosphatase (ALP, 1:750 dilution; Dako) were used as the secondary antibodies. Signals were detected with an ALP buffer containing bromo-chloro-indolyl phosphate (BCIP; Sigma-Aldrich) and nitro blue tetrazolium (NBT; Sigma-Aldrich) as substrates. Even loading was verified using a mouse monoclonal anti-tubulin antibody (1:2,000 dilution; Sigma-Aldrich). Lysates made from OLG primary cultures (see below) were dealt with the same way. A quantitative analysis of the immunoreactive bands was performed using computerized densitometry with a Scanning Imager and ImageQuant<sup>®</sup> software (Molecular Dynamics).

**Immunohistochemistry of EAE Tissue.** Grade 4 EAE and control non-EAE mice were perfused under anesthesia through the left ventricle with 4% paraformaldehyde in PBS, and the cervical, thoracic, and lumbar spinal cords were dissected. For cryosectioning, blocks of tissue were rinsed with PBS, cryoprotected in 30% sucrose in PBS overnight at 4°C, embedded in OCT compound (Tissue Tek), and frozen on dry ice. Cryostat sections (10  $\mu$ m) were cut and affixed to glass slides that were precoated with 3-aminopropyltriethoxysilane (APS; Matsunami). Samples were incubated with anti-caspase-1 antibody, anti-caspase-11 antibody, rabbit polyclonal anti-activated caspase-3, or anti-caspase-8 antibody. We also used rabbit polyclonal anti- $\pi$  form of glutathione S-transferase ( $\pi$ GST) antibody (1:500 dilution; MBL), a marker for OLGs, or mouse monoclonal anti-CD3 $\epsilon$  antibody, a marker of T cells (1:100 dilution; BD PharMingen). Samples were incubated with antibodies diluted with blocking buffer for 1 h at room temperature, then washed with PBS three times. The secondary antibodies were FITC- and rhodamine-labeled anti-rat, -rabbit, and -mouse IgGs (1:200; Chemicon). For double staining with anti- $\pi$ GST antibody and a rabbit polyclonal anti-activated caspase-3 antibody (1:500 dilution; reference 9), we cut thin cryostat sections (3  $\mu$ m) and affixed adjacent sections to the same glass slides. One section was stained with anti- $\pi$ GST antibody and the other with anti-activated caspase-3 antibody. We examined these samples with a fluorescence microscope (LSM-GB200, Olympus; and LSM-510, ZEISS). For nuclear staining, samples were incubated with 1  $\mu$ M Hoechst 33342 dye for 10 min before mounting. The nuclei of apoptotic cells were condensed and had fragmented chromatin. Counting and analysis of the proportion of caspase-positive OLGs and of the infiltrating T cells were performed in three independent visual fields in a blind fashion.

**Primary Cultures.** Primary cultures of mouse OLGs were prepared from C57BL/6 control and caspase-11 knockout mice. Embryonic day 17–18 or 0-d-old pups were decapitated and their brains were retrieved. Meninges were completely trimmed from the brain submerged in HBSS (GIBCO BRL). The brains were

minced quickly in HBSS containing a trypsin-EDTA solution (0.01% trypsin/ml and 0.1 mM EDTA; GIBCO BRL) and incubated in a CO<sub>2</sub> incubator at 37°C (5% CO<sub>2</sub>) for 5 min. Cells were spun at 1,000 rpm for 5 min in a clinical centrifuge, and the cell pellets were resuspended in DMEM containing 20% fetal bovine serum (FBS) and penicillin/streptomycin at 100 U/ml and 0.1 mg/ml, respectively. The resuspended cells were plated in 25-cm<sup>2</sup>  $\Delta$ -treated flasks (Nunc), using one flask for each brain dissociated. After 7–9 d of culture, numerous pre-O-2A progenitor clusters appeared overlying a confluent layer of astrocytes. O-2A progenitors were obtained using an immunopanning method as follows: 100-mm suspension culture dishes (Corning) were coated with 20  $\mu$ g of affinity-purified rabbit anti-rat IgG antibody (Zymed Laboratories) in 10 ml Tris buffer, pH 9.5, for 12 h at 4°C. Dishes were washed three times with PBS and incubated with rat anti-platelet-derived growth factor receptor  $\alpha$  (PDGFR $\alpha$ ) antibody (100  $\mu$ g/dish; a gift from S.-I. Nishikawa, Kyoto University, Kyoto, Japan; reference 10), a marker for O-2A progenitors, in PBS for 1 h at room temperature. Dishes were then washed twice with PBS. Suspensions of cells from the flasks were added to the panning dishes. After 1 h of incubation at room temperature, each plate was washed eight times with PBS with gentle swirling to remove nonadherent cells. The remaining adherent cells were detached by incubating with 0.25% trypsin (Difco) diluted in HBSS for 10 min at 37°C, collected by centrifugation at 1,000 rpm for 5 min, and resuspended in DMEM containing 2% FBS, antibiotics, and Bottenstein and Sato's (BS) supplement (11). BS supplement includes 0.1 mg/ml transferrin, 0.1 mg/ml BSA, 60 ng/ml progesterone, 40 ng/ml sodium selenite, 40 ng/ml thyroxine, 30 ng/ml triiodothyronine, 16  $\mu$ g/ml putrescine, and 5  $\mu$ g/ml insulin (all from Sigma-Aldrich). Cells were plated onto dishes or microcoverslips (Matsunami) coated with poly-L-lysine (mol wt >70,000; ICN Biomedicals). We also used a shaking method to obtain O-2A progenitors and mature OLGs. The caps of the flasks were tightened and the flasks were shaken by hand  $\sim$ 10–20 times. Such shaking detached O-2A progenitors into the medium; the medium from the different flasks was combined and spun at 1,000 rpm for 5 min, and the resulting pellets were resuspended in S-MEM (GIBCO BRL). Cell suspensions were spun again at 1,000 rpm for 5 min. The cell pellets were resuspend in DMEM with 2% FBS, antibiotics, and BS supplement. The suspension was passed through a glass pipette gently 30 times and plated out. At 3–5 d of culture, O-2A progenitors began to differentiate gradually into mature OLGs.

**Genotyping of Caspase-11 Knockout Mice.** Newborn mice from a breeding pair of caspase-11<sup>-/-</sup> or caspase-11<sup>+/-</sup> mice were decapitated, and whole brains were dissected. The cells of each brain were plated in one 25-cm<sup>2</sup>  $\Delta$ -treated flask (Nunc) using the primary culture procedure described above. PCR was used to genotype caspase-11 knockout mice. Genomic DNA was isolated from tails in lysis buffer (100 mM Tris-HCl, pH 8.5, 5 mM EDTA, 0.2% SDS, 200 mM NaCl, 100  $\mu$ g proteinase K/ml). The primer sequences used for the PCR were as follows: SY-21, 5'-GGCATGGAGTCAGAGATGAAAGAC-3'; SY-22, 5'-GCCCATGTGGCATTACCTGCCAGC-3'; SYKO, 5'-AGATCTACACCTCTGCACAACCTGGGGT-3'; and PJK, 5'-TGCGCTACCCGGTGGATGTGGAATGTG-3'.

The wild-type genome of *caspase-11* could be detected using SY-21 and SY-22 (an  $\sim$ 200-bp PCR product), and the mutant caspase-11 gene could be detected using SYKO and PJK (an  $\sim$ 600-bp PCR product). The following conditions were used for the PCR reaction: 1 $\times$  ExTaq PCR buffer (Takara), 0.06 mM dNTPs, 25 pmol of each primer, 0.5 U of ExTaq DNA poly-

merase (Takara) in a total volume of 20  $\mu$ l. The DNA was denatured at 94°C for 2.5 min, annealed at 55°C for 1.5 min, and elongated at 72°C for 1 min with 35 cycles.

**OLG Viability Assay.** After 48–72 h of primary culture of OLG, human recombinant TNF- $\alpha$  (200 ng/ml; Sigma-Aldrich), anti-Fas antibody (Jo2, 200 ng/ml; BD PharMingen), or recombinant mouse IFN- $\gamma$  (100 U/ml; Genzyme) were administered to each well of the mature caspase-11<sup>-/-</sup> or caspase-11<sup>+/-</sup> OLGs. After a 72-h incubation, cells were homogenized in assay buffer for immunoblotting (see above) or fixed with 4% paraformaldehyde in PBS for 10 min. The samples were washed with PBS three times, incubated with rabbit polyclonal anti-myelin basic protein (MBP) antibody (1:100 dilution; reference 12) for 1 h at room temperature, then washed with PBS three times. Samples were incubated with ALP-conjugated anti-rabbit IgG antibody for 1 h at room temperature, then washed with PBS three times. MBP was detected with an ALP buffer containing BCIP and NBT as substrates.

**ELISA for Cytokine Secretion.** The whole brain and spinal cord (cervical to lumbar) in a mouse with EAE, a postimmunization day-matched caspase-11 knockout, and an uninjected control mouse were dissected and homogenized in PBS, then frozen immediately. IL-1 $\beta$  and IFN- $\gamma$  were quantified using a mouse ELISA kit (Endogen). The absorbance was read at 450 nm with a Biolumin 960 fluorescence/absorbance microassay reader (Molecular Dynamics). The data for each cytokine were collected and analyzed in three independent measurements.

**Statistical Methods.** The results are expressed as the mean  $\pm$  SEM. The probability of statistical differences between experimental groups was determined by a Student's *t* test, as indicated.

## Results

**Expression of Caspases in the Spinal Cord of Mice with EAE.** EAE is characterized by inflammation and demyelination in the CNS. Like MS, EAE shows a perivascular inflammatory infiltration in the spinal cord and brain that is composed primarily of T cells and macrophages. We previously reported observing apoptotic OLGs in EAE lesions (3). To investigate the expression of caspases in EAE lesions, protein lysates were prepared from the upper (cervical and thoracic) and lower (lumbar) spinal cord of mice 20 d after MOG injection. Immunoblots probed with antibodies to caspase-1, -11, and -8 revealed that the expression of these caspases was strongly elevated in spinal cord lysates from EAE mice (Fig. 1 A). We also performed immunohistochemistry using antibodies against caspases. As shown in Fig. 1, B–E, the caspases were expressed in very few cells in spinal cord sections from normal control mice, but were all strongly expressed in many cells in mice with grade 4 EAE (Fig. 1, F–I). Strong immunoreactivity against caspase-1, -11, and activated caspase-3 was found at the outer surface of the spinal cord and in the white matter. Caspase-8 expression was largely confined to the outer surface of the white matter. Next, we examined immunostaining using antibodies for several caspases together with a cell type-specific marker, an antibody to the anti- $\pi$ GST, a marker for mature OLGs. Because  $\pi$ GST labeling was

more intense in the cell body and the proximal processes of mature OLGs (13, 14), we could detect and count mature OLGs more easily than by using other antibodies that label OLGs in a more general way. Together with the results of Fig. 1, F–I, our observations show that many OLGs in the white matter of the lumbar spinal cord of mice with EAE strongly expressed caspase-1, -11, and activated caspase-3, but that few expressed caspase-8 (Fig. 1, J–M).

*Caspase-1 Family Member-positive OLGs Expressed Activated Caspase-3 in the EAE Lesions.* Previously we defined that OLGs in the spinal cords of mice with severe EAE expressed caspase and some of them had undergone apoptosis (3). Approximately 10% of OLGs in the spinal

cord lesions with EAE showed apoptotic nuclear morphology (3). Since one of the hallmarks of apoptosis is the activation of caspase-3, we tested whether OLGs in EAE lesions underwent apoptosis via caspase-3 activation in the immunohistochemistry. We prepared sequential sections of lumbar spinal cord from an EAE mouse (3- $\mu$ m thick), and performed immunostaining with anti-activated caspase-3 antibody on one section and with anti- $\pi$ GST antibody on an adjacent section. We found that many OLGs in EAE lesions expressed activated caspase-3. Some of them revealed a condensed or fragmented nucleus by Hoechst 33342 nuclear staining. Then we calculated the ratio of OLGs that expressed activated caspase-3 and OLGs that showed apop-

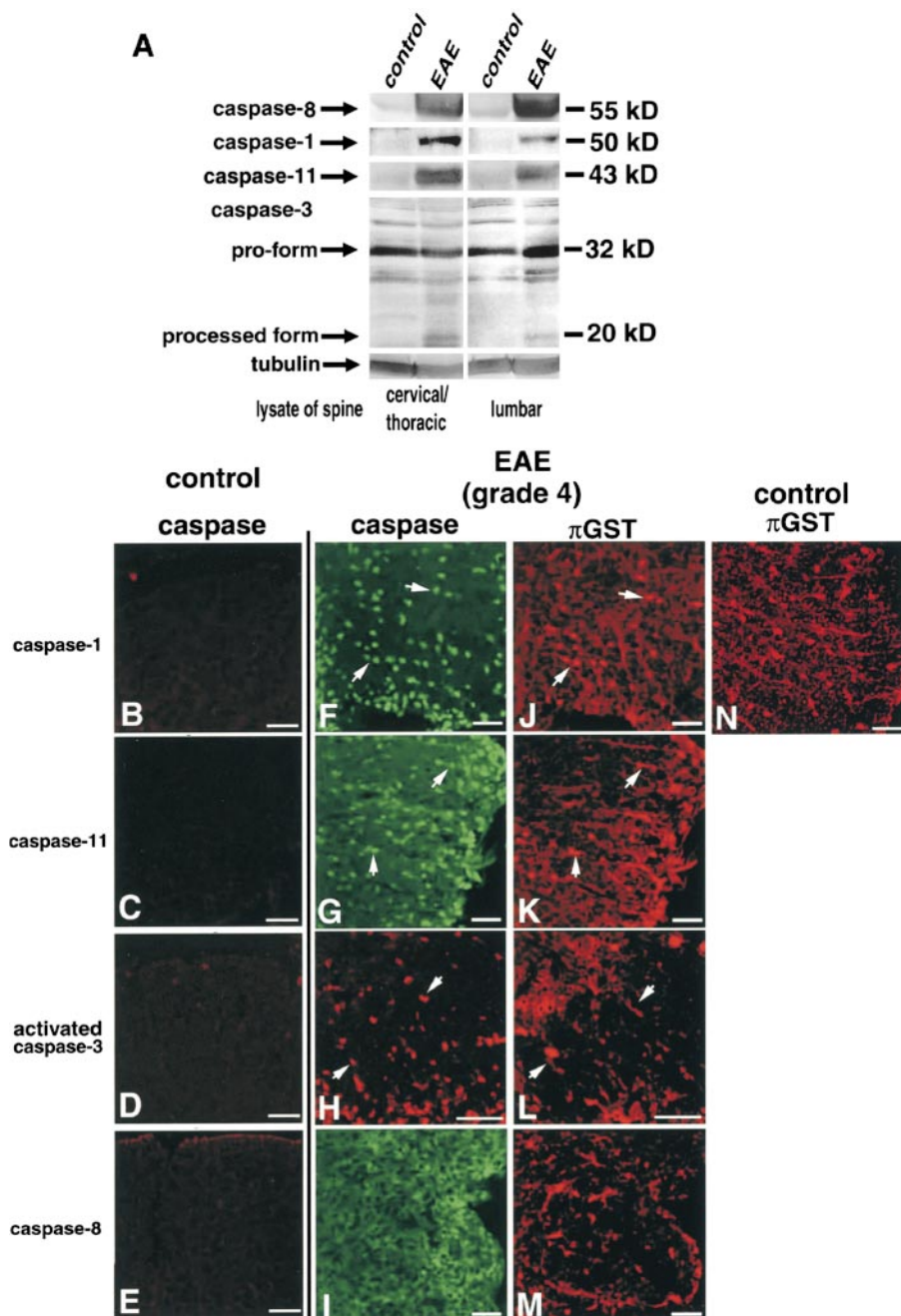


**Figure 1.** Caspases are expressed in the OLGs of the white matter of the lumbar spinal cord of mice with EAE. (A) Immunoblot analysis of the cervical/thoracic and lumbar spinal cord lysates from EAE mice using anti-caspase-8, -1, -11, and -3 antibodies. Even loading was demonstrated using an antitubulin antibody. Caspase-8, -1, and -11 were markedly induced in the lumbar/cervical and thoracic spinal cord of EAE (grade 4) mice. (B–E) Immunohistochemical analysis using anticaspase antibodies of the lumbar spinal cord from adult female uninjected control mice. Bar, 50  $\mu$ m. (F–N) Double immunohistochemical analysis of the lumbar spinal cord from EAE mice using anticaspase antibodies (F–I) and  $\pi$ GST, a specific marker of mature OLGs (J–M, from EAE mice; N, from nonEAE control mouse). Although little expression of caspase-1, -11, -8, or activated caspase-3 was detected in the normal lumbar spinal cord, these were strongly expressed in EAE mice. Caspase-8 was not expressed in  $\pi$ GST<sup>+</sup> OLGs. For double staining with anti-activated caspase-3 (H) and anti- $\pi$ GST (L) antibodies, thin cryostat sections (3  $\mu$ m) were made. One section was stained with anti- $\pi$ GST antibody and an adjacent one was stained with anti-activated caspase-3 antibody. Arrows indicate representative OLGs that express caspase-1, -11, and activated caspase-3. Bar, 50  $\mu$ m.

otic nuclear degeneration in the observation of multiple microscopic visual fields. Approximately 45% of  $\pi$ GST<sup>+</sup> OLGs expressed activated caspase-3, and 10% of OLGs showed condensed or fragmented nuclei, indicating that these cells were undergoing apoptosis (Fig. 2, A and B). The ratio of caspase-3-expressing OLGs that showed nuclear degeneration was also  $\sim$ 10%, so we concluded that almost all of the apoptotic OLGs expressed activated

caspase-3. We next compared the expression of caspase-1 subfamily members in OLGs of the spinal cord of mice with EAE. First, we calculated the ratio of OLGs that expressed caspase-1 or -11. Then we compared the ratio of activated caspase-3 expression between caspase-1- or -11-positive OLGs in the lesions of EAE. We found that many OLGs that were positive for both caspase-11 or -1 and activated caspase-3 existed in the lumbar spinal cord of EAE

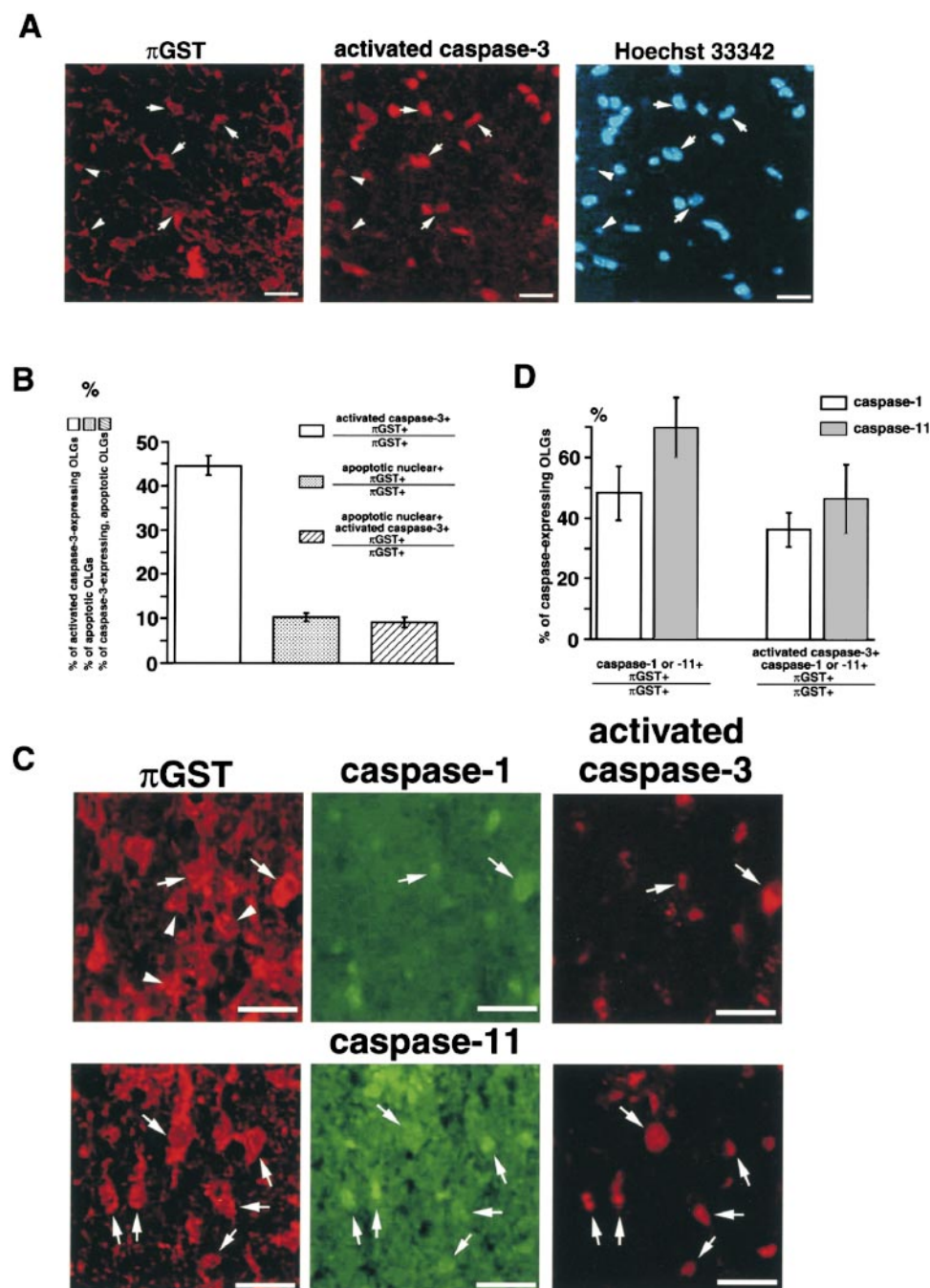


**Figure 2.** Caspase-11-positive OLGs express activated caspase-3 and undergo cell death in EAE lesions. (A) Immunohistochemical staining with anti- $\pi$ GST and anti-activated caspase-3 antibodies. The left panel shows a section of the white matter of a lumbar spinal cord from a mouse with EAE, stained with anti- $\pi$ GST antibody; the middle panel shows an adjacent section stained with anti-activated caspase-3 antibody. The right panel shows nuclear staining with Hoechst 33342. Note that many of the caspase-3-positive OLGs had an intact nucleus, as seen with Hoechst 33342 (arrow), but  $\sim$ 10% of the caspase-3-positive OLGs appeared to be apoptotic (arrowhead). Bar, 20  $\mu$ m. (B) The ratio of apoptotic OLGs in the lumbar spinal cord of EAE mice. The data give the percentage of activated caspase-3-expressing OLGs of the total number of OLGs, the percentage of apoptotic nuclear OLGs of the total number of OLGs, and the percentage of apoptotic nuclear OLGs of the total number of activated caspase-3-positive OLGs counted in three independent visual fields selected in a blind manner. Values are means  $\pm$  SEM (error bars). (C) Activated caspase-3-positive OLGs express caspase-1 and -11. One section was stained with anti- $\pi$ GST antibody and an adjacent one with anti-caspase-1 or -11 antibodies and anti-activated caspase-3 antibody. In EAE lesions,  $\pi$ GST<sup>+</sup> OLGs highly expressed caspase-1, -11, and activated caspase-3. Arrows indicate activated caspase-3-positive OLGs that also expressed caspase-1 or -11. Arrowheads indicate OLGs that expressed neither activated caspase-3 nor -1 or -11. Bar, 20  $\mu$ m. (D) Relative number of caspase-1 subfamily-positive OLGs in the white matter of the lumbar spinal cord from an EAE mouse. The data give the percentage of caspase-1- or -11-positive cells of the total number of  $\pi$ GST<sup>+</sup> cells and the percentage of activated caspase-3-positive OLGs of the total number of caspase-1- or -11-expressing OLGs counted in three independent visual fields selected in a blind manner. Values are means  $\pm$  SEM (error bars).



(Fig. 2, C and D). Approximately 50% or fewer of the OLGs in EAE lesions were caspase-1-positive and >70% were caspase-11-positive (Fig. 2 D). Approximately 50% of the activated caspase-3-positive OLGs expressed caspase-11 and ~40% of the activated caspase-3-positive OLGs expressed caspase-1. Colocalization of caspase-1 subfamily with activated caspase-3 suggests the involvement of this family member in activation of caspase-3 in OLGs.

**Caspase-11 Is Essential in Cytokine-induced OLG Cell Death.** To evaluate a possible role for caspase-11 in OLG cell death, we prepared purified OLGs as a primary culture from both wild-type and caspase-11<sup>-/-</sup> mice, and treated them with TNF- $\alpha$  or IFN- $\gamma$ . After a 72-h incubation, we made cell lysates from the cultures and used them for immunoblotting with anti-caspase antibodies. In the lysates from wild-type OLGs, the expression of caspase-1, -11, and the processed form of caspase-3 was induced by TNF- $\alpha$  and IFN- $\gamma$  (Fig. 3 A). In contrast, caspase-8 was not detected in either the cytokine-treated or the untreated ly-

sates. These results were consistent with the immunohistochemical results shown in Fig. 1, I and M. Interestingly, even though caspase-1 expression was induced by cytokines in the caspase-11<sup>-/-</sup> OLGs, the amount of processed caspase-3 was less than in wild-type OLGs. This result indicates that caspase-11 plays a more important role in activating caspase-3 than does caspase-1 in cytokine-induced OLG cell death. We next prepared purified OLGs from both caspase-11<sup>-/-</sup> and caspase-11<sup>+/-</sup> mice and treated them with TNF- $\alpha$ , IFN- $\gamma$ , or the anti-Fas antibody Jo2. After a 72-h incubation, the cells were fixed and mature OLGs were identified by staining with an anti-MBP antibody to allow us to quantify the changes in the number of OLGs. Caspase-11-deficient OLGs were almost completely resistant to the cell death induced by IFN- $\gamma$  and the anti-Fas antibody Jo2, and partially resistant to that induced by TNF- $\alpha$  (Fig. 3, B and C). These results strongly suggest that caspase-11 is involved in promoting the OLG cell death induced by cytotoxic cytokines or Fas.

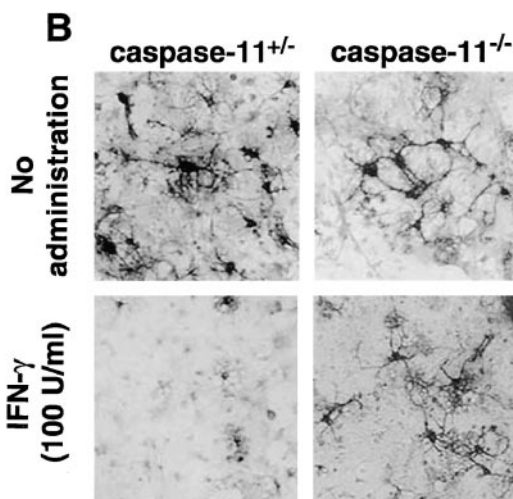
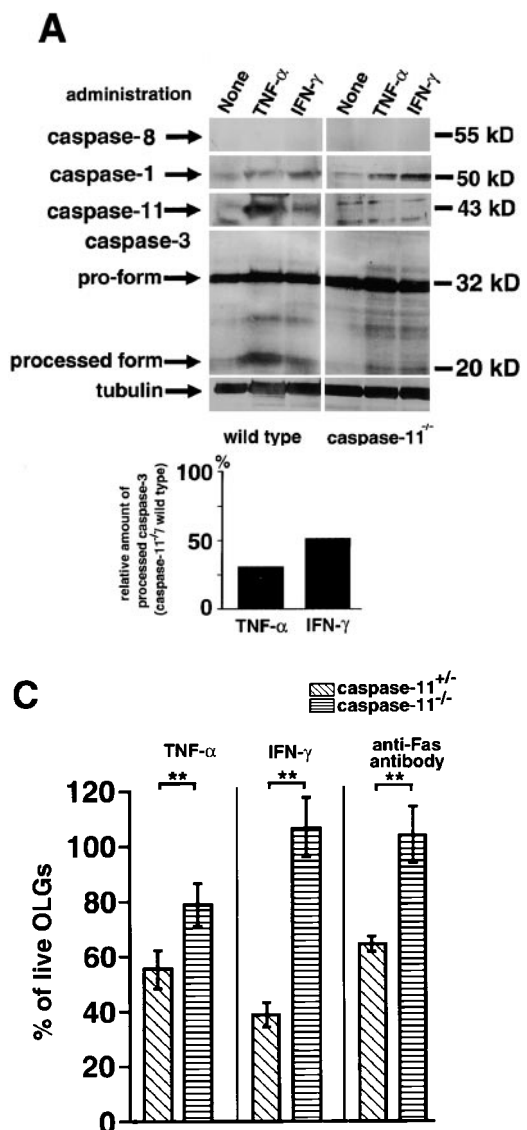
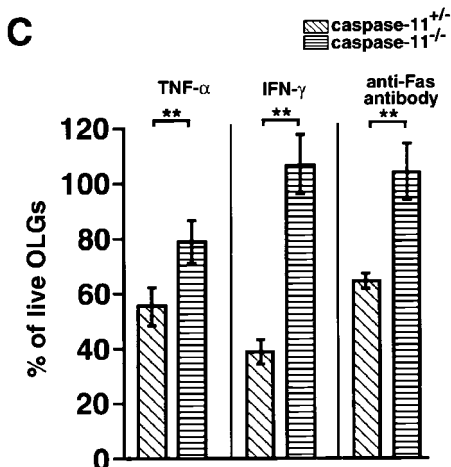


**Figure 3.** Caspase-11 plays an important role in cytokine-induced OLG cell death. (A) Immunoblot analysis of OLG lysates from wild-type control and caspase-11<sup>-/-</sup> mice using anti-caspase-1, -11, -8, and -3 antibodies. Even loading was demonstrated using an antitubulin antibody. Bar graph represents a densitometric analysis showing the relative amount of the processed caspase-3, produced by the treatment of cytokines between control and caspase-11 knockout mice, expressed as a percentage. (B) Primary cultured OLGs from caspase-11<sup>+/-</sup> and caspase-11<sup>-/-</sup> mice with or without the addition of 100 ng/ml IFN- $\gamma$ . Many MBP<sup>+</sup> OLGs from caspase-11<sup>-/-</sup> mice were observed 72 h after IFN- $\gamma$  administration. Original magnification: 100 $\times$ . (C) Percentages of cultured cells that represented live OLGs, calculated by counting MBP<sup>+</sup> OLGs. TNF- $\alpha$  (200 ng/ml), IFN- $\gamma$  (100 U/ml), and anti-Fas antibody (100 ng/ml) were administered to OLG cultures, which were fixed ~72 h later. In each experiment, the OLGs collected from each independent well were counted, and the relative percentage of MBP<sup>+</sup> cells was expressed as the mean  $\pm$  SEM (error bars). Data were collected from three independent experiments. \*\* $P < 0.01$  at each distance (Student's  $t$  test).



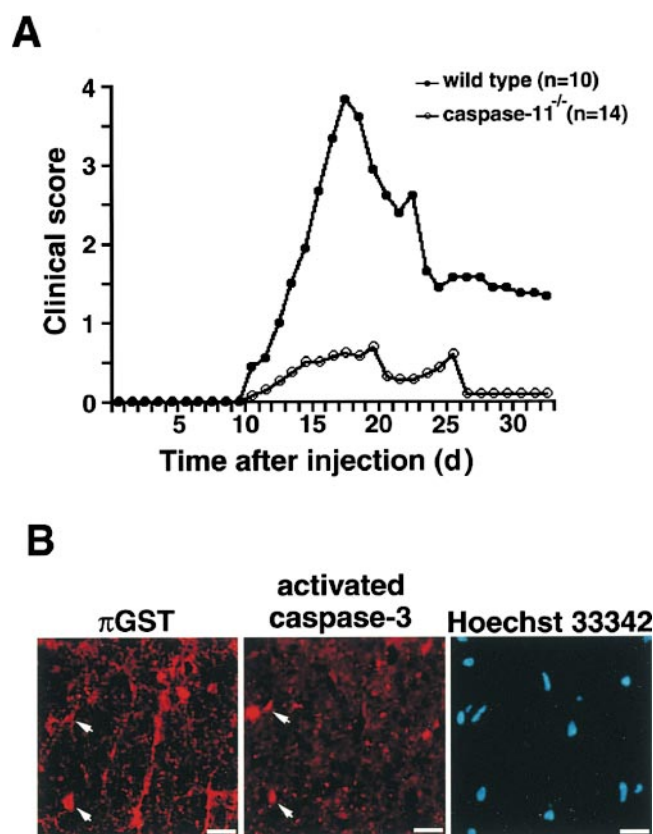
**Caspase-11-deficient Mice Are Resistant to EAE.** To further explore the role of caspase-11 in the progression of EAE, we studied the susceptibility of caspase-11<sup>-/-</sup> mice to MOG peptide-induced EAE. Most wild-type mice develop severe hind limb paralysis 20 d after rat MOG<sub>35-55</sub> peptide immunization (Fig. 4 A). The incidence of EAE in control mice was 90% (9/10), with a mean peak of clinical severity of grade 3.8 ± 0.4 (see Materials and Methods, Induction and Assessment of EAE). However, the incidence and severity of EAE in caspase-11<sup>-/-</sup> mice were significantly reduced (21% incidence, 3/14; severity: 0.679 ± 0.428; *P* < 0.001). We performed immunohistochemistry with anti- $\pi$ GST and anti-activated caspase-3 antibodies on the lumbar spinal cord from a caspase-11<sup>-/-</sup> mouse at 20 d after immunization. The number of activated caspase-3-expressing OLGs was <50% of a wild-type mouse (Fig. 4, B and C). There were very few apoptotic OLGs in the white matter of the caspase-11<sup>-/-</sup> mouse, as determined using Hoechst 33342 staining. Only <1% of OLGs showed apoptotic and expressed activated caspase-3 (Fig. 4 C). Taken together, these results indicate that caspase-11 plays a significant role in the susceptibility of OLGs to EAE induction.

**Involvement of Caspase-11 in the Production of Inflammatory Cytokines.** Caspase-1 subfamily molecules are crucially involved in immune-mediated inflammation because of their role in regulating the cellular export of cytokines such as IL-1 $\beta$  and IL-18 (15). Fig. 5, A–D, shows that CD3 $\epsilon$ <sup>+</sup>

infiltrating T cells express caspases-1 and -11. However, spinal cords from an immunized caspase-11-deficient and a nonimmunized wild-type mouse showed little or no infiltration of T cells (Fig. 5, E and F). To explore the role of caspase-11 in the cytokine production of EAE, we analyzed the concentration of several cytokines in the CNS with MOG peptide-immunized wild-type and caspase-11<sup>-/-</sup> mice. The brain and spinal cord of knockout and wild-type mice were isolated 20 d after MOG peptide injection. For controls, the tissues of an age- and sex-matched uninjected female wild-type mouse were isolated the same way. The concentrations of IL-1 $\beta$  and IFN- $\gamma$  in the lysates from these tissues were quantified by ELISA (Fig. 5 G). The amounts of these cytokines were markedly increased in the brain and spinal cord of mice with grade 4 EAE compared with samples from uninjected wild-type mice. The concentrations of these cytokines were dramatically reduced in the samples from caspase-11<sup>-/-</sup> mice. These results suggest that caspases-1 and -11 are expressed in infiltrating T cells and that the expression of caspase-11 is involved in the production of IL-1 $\beta$  and IFN- $\gamma$  in the CNS of mice with EAE.

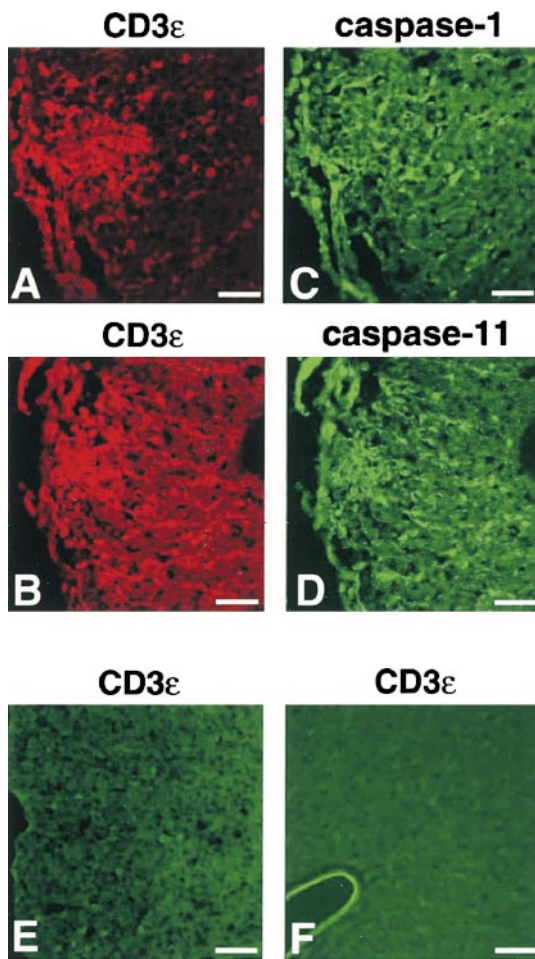
## Discussion

In this study, we show that caspase-11 plays a critical role in the susceptibility of mice to EAE induction. Caspase-



percentage of apoptotic nuclear OLGs of the total number of OLGs, and the percentage of cells showing apoptotic nuclear features of the total number of activated caspase-3-positive OLGs counted in three independent visual fields selected in a blind manner. Values are means ± SEM (error bars).

**Figure 4.** Caspase-11-deficient mice are less susceptible to EAE induction. (A) Daily mean clinical course and severity of the EAE induced by MOG<sub>35-55</sub> peptide for each genotype. Clinical signs of the disease were monitored daily, beginning on day 7, and were graded on a scale from 0 to 6. (B) Immunohistochemical staining of the white matter of the lumbar spinal cord with anti- $\pi$ GST and anti-activated caspase-3 antibodies in caspase-11<sup>-/-</sup> mice in adjacent thin sections. Nuclear staining using Hoechst 33342 was also performed. Note that the numbers of both activated caspase-3-positive OLGs were markedly less in caspase-11<sup>-/-</sup> mice than in wild-type mice with grade 4 EAE. Compare with the similar staining of wild type (Fig. 2 A). Arrows indicate OLGs that express activated caspase-3. Bars: 20  $\mu$ m. (C) The percentage of activated caspase-3-positive cells and the percentage of apoptotic OLGs in wild-type versus caspase-11<sup>-/-</sup> mice 20 d after immunization. Data give the percentage of activated caspase-3-positive cells of the total number of OLGs, the percentage of apoptotic nuclear OLGs of the total number of OLGs, and the percentage of cells showing apoptotic nuclear features of the total number of activated caspase-3-positive OLGs counted in three independent visual fields selected in a blind manner. Values are means ± SEM (error bars).



**G**

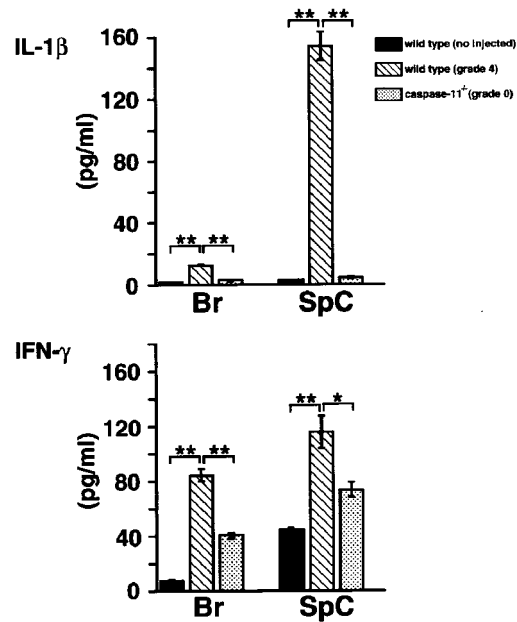


**Figure 5.** Alteration in cytokine production in the CNS of immunized caspase-11-deficient mice. (A–D) Double immunohistochemical staining with anti-CD3ε (A and B) and anti-caspase-1 or -11 (C and D) antibodies in the lumbar spinal cord of wild-type mice with grade 4 EAE. Note that the infiltrating T cells strongly expressed caspase-1 and -11. (E) The spinal cord of a caspase-11<sup>-/-</sup> mouse 20 d after immunization showed little infiltration of CD3ε<sup>+</sup> cells. (F) Immunostaining of the lumbar spinal cord with anti-CD3ε antibody in an uninjected adult female mouse. Bars, 50 μm. (G) Quantitative measurement of cytokines in the CNS by ELISA. Wild-type and caspase-11<sup>-/-</sup> mice were killed 20 d after immunization as were age- and sex-matched uninjected wild-type mice. Lysates from the brain (Br) and spinal cord (SpC) were collected and tested for IL-1β and IFN-γ, using an ELISA kit. Results are shown as the mean ± SD from three independent measurements. \*\**P* < 0.01 at each distance (Student's *t* test). \**P* < 0.05 at each distance (Student's *t* test).

11's role in OLG cell death is thought to be mediated in two ways in autoimmune demyelinating diseases. One is the so-called "cell-autonomous effect," in which processed caspase-11 in OLGs activates caspase-3 and results in cell death via specific cell death pathways. The other is the "non-cell-autonomous effect" in which caspase-11 expressed by infiltrating cells regulates the production of cytotoxic cytokines (Fig. 6). This dual role of caspase-11 may be partly responsible for the characteristic relapse and remission of autoimmune demyelinating diseases that evolve over a long period into a chronic form of disability without clear-cut exacerbation.

In a previous study, we investigated the clinical course and severity of EAE in mice that express the antiapoptotic, caspase-inhibitory protein p35 specifically in mature OLGs (3). The incidence and severity of EAE in these transgenic mice are markedly reduced (maximum clinical score of ~1.5) compared with control mice (maximum clinical score of ~4.0). Interestingly, the clinical severity of the caspase-11-deficient mice is less than that of the p35-expressing transgenic mice. As shown in Fig. 4 A, the maximum clinical score in the caspase-11 knockout mice was <1. These results suggest that absence of caspase-11 results

not only in decreasing OLG cell death but also in changing the ability of the immune system to produce cytokines that are toxic to OLGs.

It is important to discuss the role of the caspase-1 subfamily in directly killing target cells in certain diseases. We examined the cell-autonomous function of caspase-11 in the regulation of OLG cell death that was induced by treatment with TNF-α, IFN-γ, and an anti-Fas antibody. We demonstrated here that OLGs purified from caspase-11 knockout mice show complete resistance against IFN-γ and anti-Fas antibody-induced cell death (Fig. 3 C). These results suggest that caspase-11 is responsible for mediating IFN-γ- and Fas-induced OLG cell death. We could observe partial resistance against TNF-α-induced cell death in caspase-11 knockout OLGs. In this case, caspase-9/Apaf-1/cytochrome *c* pathway might also play roles in OLG cell death because we previously showed that OLG's mitochondrial membrane potential was rapidly reduced by TNF-α (16). Under pathological conditions, the expression level of activated caspase-3 was lower in caspase-11 knockout OLGs than in wild-type OLGs in vitro and in vivo (Fig. 3 A and Fig. 4, B and C). Recently, it was demonstrated that recombinant caspase-11 directly cleaves and



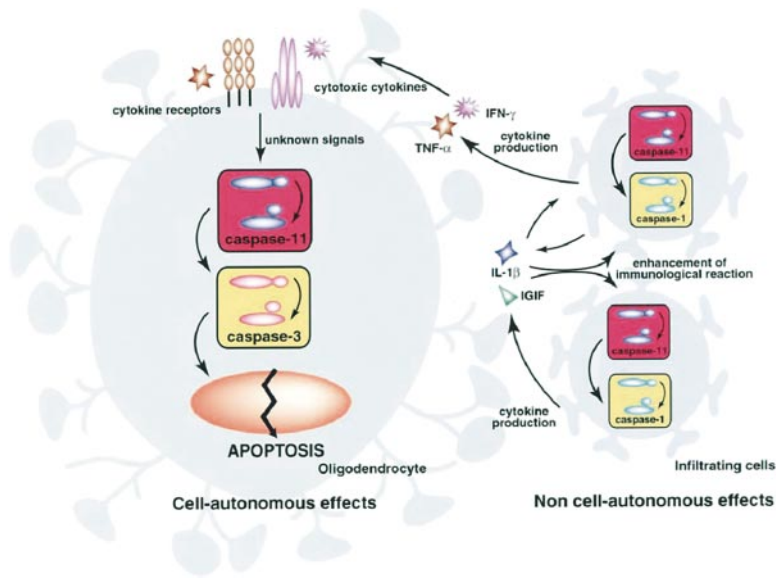


**Figure 6.** The role of caspase-11 in the pathogenesis of EAE. Caspase-11 has two effects, cell-autonomous and non-cell-autonomous. In the cell-autonomous effect, caspase-11 in OLGs is processed and activated by several unknown signals that could be derived from the stimulation of cytotoxic cytokines such as IFN- $\gamma$  and TNF- $\alpha$ . Caspase-11 activation results in OLG apoptosis via caspase-3 activation. In the non-cell-autonomous effect, caspase-11, which is a member of the caspase-1 subfamily, activates caspase-1, which regulates the maturation of cytokines, including IL-1 $\beta$  and IGIF. When inflammation occurs in the CNS, infiltrating cells from beyond the blood-brain barrier proliferate and produce cytokines that are cytotoxic to OLGs.

activates procaspase-3 *in vitro* (5). Caspase-11 preferentially cleaves the site (I/L/V/P)EHD, which is similar to sites used by upstream caspases, such as caspase-8 and -9, that activate caspase-3. All of these data strongly suggest that caspase-11 is upregulated in OLGs and activates caspase-3, leading to OLG death in EAE. Caspase-3 activation through caspase-8 or -9 is well characterized. In addition to these pathways, our data strongly suggest that a pathway involving caspases-11 and -3 seems to play important roles in certain types of pathologic cell death, including in MS and EAE. Subpopulations of neurons and OLGs in ischemic lesions strongly express caspase-11 in wild-type mice, and caspase-11-deficient mice have a reduced number of apoptotic cells and a defect in caspase-3 activation after middle cerebral artery occlusion, a mouse model of stroke (5, 17). The size of the damaged area and the resulting functional damage due to experimental ischemia are significantly reduced in caspase-1 dominant negative mutant mice (18) and by administration of caspase-1 subfamily-specific inhibitors in wild-type mice (19). These results suggest that the caspase-1 subfamily, especially caspase-11, plays a pivotal role in the pathogenesis (including executing the cell death of target cells) of not only MS and EAE but also acute progressive neurological diseases such as cerebral infarction.

Caspase-8 plays a central role in the cytokine-mediated caspase cascade. Multimerization of TNF receptors and Fas initiates the recruitment of various adapter proteins through death domain interactions; this complex directly binds to and promotes the transcatalytic activation of caspase-8 (20, 21). Whereas caspase-8 was upregulated in CNS lysates from mice with EAE (Fig. 1 A), it was not detected in OLGs that were exposed to cytotoxic cytokines in primary cultures (Fig. 4 A). In a study using rat OLGs from long-term cultures, procaspase-8 was expressed and activated after treatment with apoptotic stimuli such as staurosporine or nerve growth factor (NGF; reference 22).

However, the characteristics of OLGs differ with different culture conditions. For example, NGF does not induce OLG cell death in our cultures; rather, it prevents TNF- $\alpha$ -induced OLG cell death (16). Our *in vivo* and *in vitro* observations indicate that caspase-8 has little involvement in cytokine-induced OLG cell death in EAE because we failed to detect caspase-8 in either cultured OLGs (Fig. 3 A) or OLGs populating EAE lesions (Fig. 1, I and M).

In this study, we observed many CD3 $\epsilon^+$  T cells in the white matter of wild-type mice with severe EAE, although very few such cells were found in caspase-11 $^{-/-}$  mice (Fig. 5, A, B, and E). We previously showed that very few infiltrating cells are observed in the spinal cord lesions of EAE mice that express the antiapoptotic protein p35 in mature OLGs (3). We presume that prevention of OLG cell death inhibits inflammatory reaction and subsequent tissue injury. Inflammation is considered to be the most important cause of tissue injury in several diseases. Using a murine model of renal ischemia, administration of a caspase inhibitor and antiapoptotic agents at the time of reperfusion prevents the early onset of not only renal apoptosis but also inflammation and tissue injury (23). Treatment with a caspase-1 subfamily-specific inhibitor in the murine model of cerebral ischemia results in a significant reduction in the infarct volume and the levels of the proinflammatory cytokines IL-1 $\beta$  and TNF- $\alpha$  (24). These results strongly suggest that apoptosis of target cells is a critical event that can trigger subsequent inflammation and lead to the deterioration of the clinical manifestation of diseases due to tissue injury.

Members of the caspase-1 subfamily play important roles in both apoptosis and inflammatory responses (7, 25). We found that caspases-1 and -11 were highly expressed in CNS lesions of mice with EAE, especially in CD3 $\epsilon^+$  T cells. Caspase-1 is the protease responsible for processing proIL-1 $\beta$  to mature IL-1 $\beta$ . The IL-1 receptor antagonist (IL-1ra) inhibits the apoptosis induced by trophic factor deprivation in primary neurons, as well as by TNF- $\alpha$  in fi-

broblasts (26). Treatment with rhIL-1ra during the effector phase of EAE significantly reduces the clinical signs of EAE (27). IL-1 is a potent mitogen for astroglia but has no effect on OLGs, suggesting that IL-1, released by inflammatory cells, may promote the formation of astroglial scars in the damaged mammalian brain (28). It is possible that IL-1 $\beta$  released by infiltrating macrophages promotes gliosis and the progression of MS.

Previous studies revealed that caspase-1 can also process proIFN- $\gamma$  inducing factor (proIGIF or proIL-18), thereby regulating the production of IFN- $\gamma$ , which is involved in the pathogenesis of inflammatory processes (15, 29). IFN- $\gamma$  and TNF- $\alpha$  are also involved in reactive astroglia (30). The cytotoxicity of microglia for OLGs can be enhanced by IFN- $\gamma$  and blocked by an anti-TNF- $\alpha$  antibody (31). A single microinjection of TNF- $\alpha$  or IFN- $\gamma$  into the lumbosacral spinal cord of rats produces an inflammatory response with a remarkably similar pattern to that observed during EAE (32). IFN- $\gamma$  and IL-1 $\beta$  alone do not induce TNF- $\alpha$  production from astrocytes; however, combined treatment with IFN- $\gamma$  and IL-1 $\beta$  results in a striking synergistic effect on astrocyte TNF- $\alpha$  production (33). It is possible that activated caspase-1 and -11 in infiltrating CD3 $\epsilon^+$  T lymphocytes mediate the production of IL-1 $\beta$  and IFN- $\gamma$ , and that these cytokines mediate their cytotoxicity against the OLGs in EAE lesions through TNF- $\alpha$ . By activating caspase-1, caspase-11 is likely to promote OLG cell death through the production of cytokines, and thereby to elicit their effects in a non-cell-autonomous manner (Fig. 6).

The role of cytokine in the pathogenesis of autoimmune-mediated demyelinating diseases including EAE is still unclear and the cytotoxic effect against OLG in the lesion of diseases is controversial. In an in vitro study, cultured OLGs undergo cell death induced by cytokines such as TNF- $\alpha$ , IFN- $\gamma$ , and lymphotoxin (12, 34–36). Although these results indicate that cytokines play a critical role for cytotoxicity of OLG, some previous reports show that some of them are not essential in an in vivo study for the induction and expression of inflammatory and demyelinating lesions. Mice lacking both TNF- $\alpha$  and lymphotoxin- $\alpha$  (37) or lacking TNF- $\alpha$  (38) develop severe neurological impairment with high mortality and extensive inflammation and demyelination. Mice lacking IFN- $\gamma$  receptor also develop EAE with high morbidity and mortality with severe inflammation and demyelination of the CNS (39). These observations suggest that these cytokines are potent protective for inflammation and demyelination. However, Dowling et al. (2) used the in situ TdT-mediated dUTP nick end labeling (TUNEL) technique and indicated that 14–40% of the dying cells in the acute and chronic MS plaques were OLG; there is little evidence that cytokines directly kill OLGs in demyelinating diseases. It is possible that cytokines play different roles in the various periods, such as the initiation and progression of autoimmune demyelinating diseases, so further experiments are required to elucidate the precise mechanisms of cytokines involved in producing the inflammation and demyelination.

Caspase-11 is required for the activation of caspase-1 (7). Recently, a reduction in MOG peptide-induced EAE incidence and severity was reported in caspase-1 knockout mice (4). However, we found that the caspase-1-deficient mice used in this study (40) are also deficient in their expression of caspase-11, for unknown reasons (5). Our caspase-11 $^{-/-}$  mice, which are in a C57BL/6 background, definitely express caspase-1 (Fig. 4 A), so we have confirmed that the reduced incidence and severity of EAE and lowered production of cytokines result from caspase-11 depletion. Thus, treatment with caspase-11 inhibitors could be a useful therapy for MS and other diseases in which inflammation and cell death play a role.

We thank Drs. Shinichi Nishikawa and Joseph L. Goldstein for providing us with the anti-PDGFR $\alpha$  antibody and anti-caspase-3 antibody, respectively.

This work was supported by Grants-in-Aid from the Ministry of Education, Science, and Culture to M. Miura (12031214) and H. Okano (12215090); by grants from the Human Frontier Science Program to H. Okano (RG-164/98); and by the Core Research for Evolutional Science and Technology (CREST) of the Japan Science and Technology Corporation (00371).

Submitted: 5 September 2000

Revised: 15 November 2000

Accepted: 22 November 2000

## References

1. Pender, M.P., K.B. Nguyen, P.A. McCombe, and J.F. Kerr. 1991. Apoptosis in the nervous system in experimental allergic encephalomyelitis. *J. Neurol. Sci.* 104:81–87.
2. Dowling, P., W. Husar, J. Menonna, H. Donnenfeld, S. Cook, and M. Sidhu. 1997. Cell death and birth in multiple sclerosis brain. *J. Neurol. Sci.* 149:1–11.
3. Hisahara, S., T. Araki, F. Sugiyama, K. Yagami, M. Suzuki, K. Abe, K. Yamamura, J. Miyazaki, T. Momoi, T. Saruta, et al. 2000. Targeted expression of baculovirus p35 caspase inhibitor in oligodendrocytes protects mice against autoimmune-mediated demyelination. *EMBO (Eur. Mol. Biol. Organ.) J.* 19:341–348.
4. Furlan, R., G. Martino, F. Galbiati, P.L. Poliani, S. Smirondo, A. Bergami, G. Desina, G. Comi, R. Flavell, M.S. Su, et al. 1999. Caspase-1 regulates the inflammatory process leading to autoimmune demyelination. *J. Immunol.* 163:2403–2409.
5. Kang, S.J., S. Wang, H. Hara, E.P. Peterson, S. Namura, S. Amin-Hanjani, Z. Huang, A. Srinivasan, K.J. Tomaselli, N.A. Thornberry, et al. 2000. Dual role of caspase-11 in mediating activation of caspase-1 and caspase-3 under pathological conditions. *J. Cell Biol.* 149:613–622.
6. Wang, S., M. Miura, Y. Jung, H. Zhu, V. Gagliardini, L. Shi, A.H. Greenberg, and J. Yuan. 1996. Identification and characterization of Ich-3, a member of the interleukin-1 $\beta$  converting enzyme (ICE)/Ced-3 family and an upstream regulator of ICE. *J. Biol. Chem.* 271:20580–20587.
7. Wang, S., M. Miura, Y.K. Jung, H. Zhu, E. Li, and J. Yuan. 1998. Murine caspase-11, an ICE-interacting protease, is essential for the activation of ICE. *Cell.* 92:501–509.
8. Wang, X., N.G. Zelenski, J. Yang, J. Sakai, M.S. Brown, and J.L. Goldstein. 1996. Cleavage of sterol regulatory element binding proteins (SREBPs) by CPP32 during apoptosis.

- EMBO (Eur. Mol. Biol. Organ.)*. 15:1012–1020.
9. Kouroku, Y., K. Urase, E. Fujita, K. Isahara, Y. Ohsawa, Y. Uchiyama, M.Y. Momoi, and T. Momoi. 1998. Detection of activated caspase-3 by a cleavage site-directed antiserum during naturally occurring DRG neurons apoptosis. *Biochem. Biophys. Res. Commun.* 247:780–784.
  10. Takakura, N., H. Yoshida, T. Kunisada, S. Nishikawa, and S.I. Nishikawa. 1996. Involvement of platelet-derived growth factor receptor- $\alpha$  in hair canal formation. *J. Invest. Dermatol.* 107:770–777.
  11. Hall, A., N.A. Giese, and W.D. Richardson. 1996. Spinal cord oligodendrocytes develop from ventrally derived progenitor cells that express PDGF $\alpha$ -receptors. *Development.* 122:4085–4094.
  12. Hisahara, S., S. Shoji, H. Okano, and M. Miura. 1997. ICE/CED-3 family executes oligodendrocyte apoptosis by tumor necrosis factor. *J. Neurochem.* 69:10–20.
  13. Tansey, F.A., and W. Cammer. 1991. A pi form of glutathione-S-transferase is a myelin- and oligodendrocyte-associated enzyme in mouse brain. *J. Neurochem.* 57:95–102.
  14. Cammer, W., and H. Zhang. 1992. Localization of Pi class glutathione-S-transferase in the forebrains of neonatal and young rats: evidence for separation of astrocytic and oligodendrocytic lineages. *J. Comp. Neurol.* 321:40–45.
  15. Gu, Y., K. Kuida, H. Tsutsui, G. Ku, K. Hsiao, M.A. Fleming, N. Hayashi, K. Higashino, H. Okamura, K. Nakanishi, et al. 1997. Activation of interferon- $\gamma$  inducing factor mediated by interleukin-1 $\beta$  converting enzyme. *Science.* 275:206–209.
  16. Takano, R., S. Hisahara, K. Namikawa, H. Kiyama, H. Okano, and M. Miura. 2000. Nerve growth factor protects oligodendrocytes from tumor necrosis factor- $\alpha$ -induced injury through Akt-mediated signaling mechanisms. *J. Biol. Chem.* 275:16360–16365.
  17. Shibata, M., S. Hisahara, H. Hara, T. Yamawaki, Y. Fukuuichi, J. Yuan, H. Okano, and M. Miura. 2000. Caspases determine the vulnerability of oligodendrocytes in the ischemic brain. *J. Clin. Invest.* 106:643–653.
  18. Friedlander, R.M., V. Gagliardini, H. Hara, K.B. Fink, W. Li, G. MacDonald, M.C. Fishman, A.H. Greenberg, M.A. Moskowitz, and J. Yuan. 1997. Expression of a dominant negative mutant of interleukin-1 $\beta$  converting enzyme in transgenic mice prevents neuronal cell death induced by trophic factor withdrawal and ischemic brain injury. *J. Exp. Med.* 185:933–940.
  19. Hara, H., R.M. Friedlander, V. Gagliardini, C. Ayata, K. Fink, Z. Huang, M. Shimizu-Sasamata, J. Yuan, and M.A. Moskowitz. 1997. Inhibition of interleukin 1 $\beta$  converting enzyme family proteases reduces ischemic and excitotoxic neuronal damage. *Proc. Natl. Acad. Sci. USA.* 94:2007–2012.
  20. Boldin, M.P., T.M. Goncharov, Y.V. Goltsev, and D. Wallach. 1996. Involvement of MACH, a novel MORT1/FADD-interacting protease, in Fas/APO-1- and TNF receptor-induced cell death. *Cell.* 85:803–815.
  21. Muzio, M., A.M. Chinnaiyan, F.C. Kischkel, K. O'Rourke, A. Shevchenko, J. Ni, C. Scaffidi, J.D. Bretz, M. Zhang, R. Gentz, et al. 1996. FLICE, a novel FADD-homologous ICE/CED-3-like protease, is recruited to the CD95 (Fas/APO-1) death-inducing signaling complex. *Cell.* 85:817–827.
  22. Gu, C., P. Casaccia-Bonnel, A. Srinivasan, and M.V. Chao. 1999. Oligodendrocyte apoptosis mediated by caspase activation. *J. Neurosci.* 19:3043–3049.
  23. Daemen, M.A., C. van't Veer, G. Denecker, V.H. Heemskerck, T.G. Wolfs, M. Clauss, P. Vandenabeele, and W.A. Buurman. 1999. Inhibition of apoptosis induced by ischemia-reperfusion prevents inflammation. *J. Clin. Invest.* 104:541–549.
  24. Rabuffetti, M., C. Sciorati, G. Tarozzo, E. Clementi, A.A. Manfredi, and M. Beltramo. 2000. Inhibition of caspase-1-like activity by Ac-Tyr-Val-Ala-Asp-chloromethyl ketone induces long-lasting neuroprotection in cerebral ischemia through apoptosis reduction and decrease of proinflammatory cytokines. *J. Neurosci.* 20:4398–4404.
  25. Thornberry, N.A., T.A. Rano, E.P. Peterson, D.M. Rasper, T. Timkey, M. Garcia-Calvo, V.M. Houtzager, P.A. Nordstrom, S. Roy, J.P. Vaillancourt, et al. 1997. A combinatorial approach defines specificities of members of the caspase family and granzyme B. Functional relationships established for key mediators of apoptosis. *J. Biol. Chem.* 272:17907–17911.
  26. Friedlander, R.M., V. Gagliardini, R.J. Rotello, and J. Yuan. 1996. Functional role of interleukin 1 $\beta$  (IL-1 $\beta$ ) in IL-1 $\beta$ -converting enzyme-mediated apoptosis. *J. Exp. Med.* 184:717–724.
  27. Martin, D., and S.L. Near. 1995. Protective effect of the interleukin-1 receptor antagonist (IL-1ra) on experimental allergic encephalomyelitis in rats. *J. Neuroimmunol.* 61:241–245.
  28. Giulian, D., and L.B. Lachman. 1985. Interleukin-1 stimulation of astroglial proliferation after brain injury. *Science.* 228:497–499.
  29. Ghayur, T., S. Banerjee, M. Hugunin, D. Butler, L. Herzog, A. Carter, L. Quintal, L. Sekut, R. Talanian, M. Paskind, et al. 1997. Caspase-1 processes IFN- $\gamma$ -inducing factor and regulates LPS-induced IFN- $\gamma$  production. *Nature.* 386:619–623.
  30. Balasingam, V., T. Tejada-Berges, E. Wright, R. Bouckova, and V.W. Yong. 1994. Reactive astrogliosis in the neonatal mouse brain and its modulation by cytokines. *J. Neurosci.* 14:846–856.
  31. Peck, R., M. Brockhaus, and J.R. Frey. 1989. Cell surface tumor necrosis factor (TNF) accounts for monocyte- and lymphocyte-mediated killing of TNF-resistant target cells. *Cell. Immunol.* 122:1–10.
  32. Simmons, R.D., and D.O. Willenborg. 1990. Direct injection of cytokines into the spinal cord causes autoimmune encephalomyelitis-like inflammation. *J. Neurol. Sci.* 100:37–42.
  33. Chung, I.Y., and E.N. Benveniste. 1990. Tumor necrosis factor- $\alpha$  production by astrocytes. Induction by lipopolysaccharide, IFN- $\gamma$ , and IL-1 $\beta$ . *J. Immunol.* 144:2999–3007.
  34. Louis, J.C., E. Magal, S. Takayama, and S. Varon. 1993. CNTF protection of oligodendrocytes against natural and tumor necrosis factor-induced death. *Science.* 259:689–692.
  35. Vartanian, T., Y. Li, M. Zhao, and K. Stefansson. 1995. Interferon- $\gamma$ -induced oligodendrocyte cell death: implications for the pathogenesis of multiple sclerosis. *Mol. Med.* 1:732–743.
  36. Selmaj, K., C.S. Raine, M. Farooq, W.T. Norton, and C.F. Brosnan. 1991. Cytokine cytotoxicity against oligodendrocytes. Apoptosis induced by lymphotoxin. *J. Immunol.* 147:1522–1529.
  37. Frei, K., H.P. Eugster, M. Bopst, C.S. Constantinescu, E. Lavi, and A. Fontana. 1997. Tumor necrosis factor  $\alpha$  and lymphotoxin  $\alpha$  are not required for induction of acute experimental autoimmune encephalomyelitis. *J. Exp. Med.* 185:2177–2182.
  38. Liu, J., M.W. Marino, G. Wong, D. Grail, A. Dunn, J. Betadapura, A.J. Slavin, L. Old, and C.C. Bernard. 1998. TNF

- is a potent anti-inflammatory cytokine in autoimmune-mediated demyelination. *Nat. Med.* 4:78–83.
39. Willenborg, D.O., S. Fordham, C.C. Bernard, W.B. Cowden, and I.A. Ramshaw. 1996. IFN- $\gamma$  plays a critical down-regulatory role in the induction and effector phase of myelin oligodendrocyte glycoprotein-induced autoimmune encephalomyelitis. *J. Immunol.* 157:3223–3227.
40. Kuida, K., J.A. Lippke, G. Ku, M.W. Harding, D.J. Livingston, M.S. Su, and R.A. Flavell. 1995. Altered cytokine export and apoptosis in mice deficient in interleukin-1 $\beta$  converting enzyme. *Science.* 267:2000–2003.